

See discussions, stats, and author profiles for this publication at: <https://www.researchgate.net/publication/276921500>

Cucurbit[6]uril: A Possible Host for Noble Gas Atoms

ARTICLE *in* THE JOURNAL OF PHYSICAL CHEMISTRY B · MAY 2015

Impact Factor: 3.3

CITATION

1

READS

36

3 AUTHORS, INCLUDING:



Sudip Pan

IIT Kharagpur

43 PUBLICATIONS 211 CITATIONS

[SEE PROFILE](#)



Subhajit Mandal

IIT Kharagpur

9 PUBLICATIONS 10 CITATIONS

[SEE PROFILE](#)

Cucurbit[6]uril: A Possible Host for Noble Gas Atoms

Sudip Pan, Subhajit Mandal, and Pratim Kumar Chattaraj

J. Phys. Chem. B, Just Accepted Manuscript • DOI: 10.1021/acs.jpcb.5b01396 • Publication Date (Web): 19 May 2015

Downloaded from <http://pubs.acs.org> on May 19, 2015

Just Accepted

"Just Accepted" manuscripts have been peer-reviewed and accepted for publication. They are posted online prior to technical editing, formatting for publication and author proofing. The American Chemical Society provides "Just Accepted" as a free service to the research community to expedite the dissemination of scientific material as soon as possible after acceptance. "Just Accepted" manuscripts appear in full in PDF format accompanied by an HTML abstract. "Just Accepted" manuscripts have been fully peer reviewed, but should not be considered the official version of record. They are accessible to all readers and citable by the Digital Object Identifier (DOI®). "Just Accepted" is an optional service offered to authors. Therefore, the "Just Accepted" Web site may not include all articles that will be published in the journal. After a manuscript is technically edited and formatted, it will be removed from the "Just Accepted" Web site and published as an ASAP article. Note that technical editing may introduce minor changes to the manuscript text and/or graphics which could affect content, and all legal disclaimers and ethical guidelines that apply to the journal pertain. ACS cannot be held responsible for errors or consequences arising from the use of information contained in these "Just Accepted" manuscripts.



ACS Publications

High quality. High impact.

The Journal of Physical Chemistry B is published by the American Chemical Society.

1155 Sixteenth Street N.W., Washington, DC 20036

Published by American Chemical Society. Copyright © American Chemical Society.

However, no copyright claim is made to original U.S. Government works, or works produced by employees of any Commonwealth realm Crown government in the course of their duties.

1
2
3
4
5
6
7
8
9
10
11
12
13
14
15
16
17
18
19
20
21
22
23
24
25
26
27
28
29
30
31
32
33
34
35
36
37
38
39
40
41
42
43
44
45
46
47
48
49
50
51
52
53
54
55
56
57
58
59
60
Revised MS No. jp-2015-01396m.R1

Cucurbit[6]uril: A Possible Host for Noble Gas Atoms

Sudip Pan, Subhajit Mandal and Pratim K. Chattaraj*

Department of Chemistry and Centre for Theoretical Studies

Indian Institute of Technology Kharagpur, 721302, India

* Corresponding author: pkc@chem.iitkgp.ernet.in

Abstract

Density functional and ab initio molecular dynamics studies are carried out to investigate the stability of noble gas encapsulated cucurbit[6]uril (CB[6]) systems. Interaction energy, dissociation energy and dissociation enthalpy are calculated to understand the efficacy of CB[6] in encapsulating noble gas atoms. CB[6] could encapsulate up to three Ne atoms having dissociation energy (zero-point energy corrected) in the range of 3.4-4.1 kcal/mol whereas due to larger size, only one Ar or Kr atom encapsulated analogues would be viable. The dissociation energy value for the second Ar atom is only 1.0 kcal/mol. On the other hand, the same for the second Kr is -0.5 kcal/mol implying the instability of the system. The noble gas dissociation processes are endothermic in nature, which increases gradually along Ne to Kr. Kr encapsulated analogue is found to be viable at room temperature. However, low temperature is needed for Ne and Ar encapsulated analogues. The temperature-pressure phase diagram highlights the region in which association and dissociation processes of Kr@CB[6] would be favorable. At ambient temperature and pressure, CB[6] may be used as an effective noble gas carrier. Wiberg bond indices, non covalent interaction indices, electron density and energy decomposition analyses are used to explore the nature of interaction between noble gas atoms and CB[6]. Dispersion interaction is found to be the most important term in the attraction energy. Ne and Ar atoms in one Ng entrapped analogues are found to stay inside the cavity of CB[6] throughout the simulation at 298 K. However, during simulation Ng₂ units in Ng₂@CB[6] flip towards the open faces of CB[6]. After 1 ps, one Ne atom of Ne₃@CB[6] almost reaches the open face keeping other two Ne atoms inside. At lower temperature (77 K), all the Ng atoms in Ng_n@CB[6] remain well inside the cavity of CB[6] throughout the simulation time (1 ps).

Keywords: Host-guest interaction, dissociation energy, non covalent interaction, electron density analysis, energy decomposition analysis, dispersion energy

Introduction

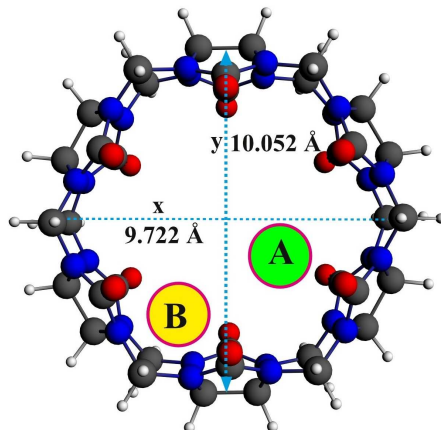
Cucurbit[*n*]urils, generally abbreviated as CBs[*n*], are macro-cyclic molecules in which *n* number of glycoluril [=C₄H₂N₄O₂=] units are connected through methylene linkages. Behrend *et al.*¹ were the first to successfully synthesize cucurbiturils in 1905, by condensing the mixture of glycoluril and formaldehyde. However, in 1981 Freeman *et al.*² elucidated their crystallographic structures. CBs[*n*] possess pumpkin-like structural design with a hydrophobic interior cavity similar to cyclodextrins and calixarenes.^{3,4} The most important feature of this CBs[*n*] family is that depending on the cavity size they could host different sizes of guest molecules.⁵ Numerous complexes with guests like anticancer drugs,³ organic dyes,⁶ viologens,⁷ metal cations,^{8,9} protonated alkyl and arylamines^{10,11} were synthesized. Even, the encapsulation of CB[5] by CB[10] was also found to be possible.¹² In addition, CB[7] was found to be effective in storing hydrogen¹³ and some other gases.¹⁴⁻¹⁶ In fact, Tian *et al.*¹⁶ reported that CB[7] could entrap CO₂ selectively over N₂ and CH₄.

The chemistry of noble gas (Ng) compounds¹⁷⁻⁴¹ is one of the fast developing fields in the recent time. The interest in the endohedrally confined Ng atoms has grown with the reporting of Ng_n@C₆₀ and Ng_n@C₇₀ compounds, both via theoretical and experimental studies.⁴²⁻⁵² Techniques involving molecular beams or shooting of Ng atoms are generally used to incorporate Ng atoms within fullerene cages.⁵³ Ng inclusion into much smaller cages like dodecahedrane,⁵⁴ adamantane,⁵⁵⁻⁵⁷ cubane and other hydrocarbon cages,⁵⁸ Mo₆Cl₈F₆,⁵⁹ B₁₂N₁₂,⁶⁰ and B₁₆N₁₆⁶⁰ was also studied. In fact, Cross *et al.*⁶¹ experimentally synthesized He@C₂₀H₂₀ despite its less stability by 33.8 kcal/mol compared to the free C₂₀H₂₀ and He atom.⁵⁴ Most of the Ng encapsulated cage compounds are thermodynamically unstable with respect to dissociation, but they are kinetically stable enough to persist since several bonds should be broken to open a window for them.^{44,54-62}

The possibility of formation of Ng-Ng covalent bonds due to the confinement was also investigated. Frenking *et al.*⁶³ made quantum-chemical calculations on Ng dimers (Ng₂) (Ng=He-Xe) confined in C₆₀ cages and found shorter Ng-Ng bond distances than those in the free dimers. They concluded Xe-Xe bond as a genuine covalent bond.⁶³ On the other hand, Ng-Ng bond could be treated as only of weak non-covalent type in cases

of lighter atoms like He and Ne.⁶³ Merino and coworkers⁶⁴ further adopted smaller cage, C₂₀H₂₀ to examine whether confinement can induce a chemical bond between two He atoms. Very recently Chakraborty *et al.*⁶⁵ studied the confinement induced binding interaction between Ng atoms inside BN-doped (3, 3) single walled carbon nanotube.

Here, keeping both the cavity size and computational economy in mind, we have considered CB[6] (structure **1**) from the CBs[n] family as a case study to explore its Ng encapsulating capability. CB[6] is also reported to be a suitable candidate for acting as a host for different guest molecules. Different thiols and disulfides,⁶⁶ ω -amino acids,⁶⁷ ω -amino alcohols,⁶⁷ bipyridine derivatives,⁶⁸ different aliphatic alcohols, acids, and nitriles,⁶⁹ aromatic compounds,^{70,71} non-ionic surfactants,⁷² etc. were found to make stable complexes with CB[6]. Further, Ghosh and coworkers^{73,74} studied complexation of CB[6] with halide ion and solvated chromate ion. The current study becomes more relevant as cucurbiturils have already been synthesized.



Structure **1**

Despite the inertness of Ng atoms, we have found that Ng atoms are bound endohedrally having reasonably large dissociation energy. CB[6] could entrap up to three Ne atoms whereas for Ar and Kr, due to their larger sizes, encapsulation up to two Ng atoms is possible. The nature of interaction between Ng and CB[6] as well as between Ng and Ng is understood by the electron density analysis,⁷⁵ energy decomposition analysis⁷⁶ (EDA) and the analysis of non covalent interaction (NCI)⁷⁷ indices and electron localization function (ELF).⁷⁸ Ab initio molecular dynamics simulation⁷⁹⁻⁸² is performed at 298 K and 77 K to examine the kinetic stability of the Ng encapsulated systems.

Computational details

The molecular geometries of CB[6] and its Ng encapsulated analogues are optimized at the ω B97X-D⁸³/6-311G(2d,p) level by using Gaussian 09 program package.⁸⁴ Harmonic vibrational frequencies are also computed at the same level to ensure the existence of the studied systems at minima on the respective potential energy surfaces (PES). Ideal gas equation is used to calculate PV appearing in the expression for the Gibbs free energy (G). The atomic charges (q) are calculated by adopting a natural population analysis (NPA) scheme. The atoms-in-molecules (AIM)⁷⁵ analysis is carried out by using the Multiwfn software⁸⁵ at the ω B97X-D/6-311G(2d,p) level. The EDA⁷⁶ is carried out at the SSB-D⁸⁶/DZP// ω B97X-D/6-311G(2d,p) level using ADF(2013.01) program package.⁸⁷

NCI⁷⁷ index is employed for analyzing the real space characteristics of the interaction. The approach for the mapping of localized binding interaction in NCI includes two scalar quantities, viz., electron density (ρ), and reduced density gradient (s), which are inter-connected as

$$s = \frac{1}{2(3\pi^2)^{1/3}} \frac{|\nabla\rho|}{\rho^{4/3}} \quad (1)$$

where $\nabla\rho$ is the gradient of ρ .

To describe the nature of bonding, the sign of $\nabla^2\rho$ is an important tool. While negative value of $\nabla^2\rho$ signifies charge accumulation (covalent bond) in between two bonded atoms, the positive sign implies charge depletion in between the same (non-covalent bond). In fact, the nature of bonding could be best described by the phenomenon of charge accumulation or depletion in a plane perpendicular to that of the interaction. Hence, the second eigenvalue (λ_2) of electron-density Hessian matrix should be taken into account.

Using the three components along the three principal axes of the maximal variation, $\nabla^2\rho$ can be decomposed into three eigenvalues (λ_i) of electron-density Hessian matrix as

$$\nabla^2\rho = \lambda_1 + \lambda_2 + \lambda_3 \quad (2)$$

For the bonding interaction such as H-bond, $\lambda_2 < 0$ and for the non-bonded interaction like steric repulsion, $\lambda_2 > 0$. On the other hand, for van der Waals type of interaction, $\lambda_2 \lesssim 0$. As the sign of λ_2 ($\text{sign}(\lambda_2)$) describes the nature of the interaction, s is plotted versus the product of $\text{sign}(\lambda_2)$ and ρ . A visualization of the gradient isosurface in real space could be made by using NCIPILOT program.⁸⁸ The value of $\text{sign}(\lambda_2)\rho$ is used to decide the color of the isosurfaces. Blue, green and red color codes are generally used to describe stabilizing H-bonding, van der Waals and destabilizing steric interaction, respectively. In the present case, a density cutoff of $\rho = 0.20$ au is applied and the pictures are generated for an isosurface value of $s = 0.5$.

The dynamics of all the Ng encapsulated CB[6] systems are studied by using an ab initio molecular dynamics,⁷⁹ atom-centered density matrix propagation (ADMP)⁸⁰⁻⁸² technique as implemented in Gaussian 09 program package.⁸⁴ The dynamics are performed at the DFT-D-B3LYP/6-31G(d)// ω B97X-D/6-311G(2d,p) level. The initial nuclear kinetic energies of the systems are generated by using a Boltzmann distribution. A velocity scaling thermostat maintains the temperature throughout the simulation. Here, we have performed all the simulations at 298 K and 77 K up to 1 ps with an 1 fs time step. Default random number generator seed is used as implemented in Gaussian 09 to obtain the initial mass weighted Cartesian velocities.

Geometries and reaction energies

The optimized geometries of the $\text{Ng}_n@\text{CB}[6]$ systems are depicted in Figure 1. We have first started free optimization followed by frequency calculation putting Ng atoms in two different places, one being in front of the $-\text{C}_4\text{H}_2\text{N}_4\text{O}_2-$ moiety (position A in structure 1) and another being in front of the $-\text{C}_2\text{H}_4\text{N}_2-$ moiety (position B in structure 1).⁸⁹ Except for $\text{Kr}@CB[6]$, the Ng trapped analogues at the A position of CB[6] appear as transition states or even higher order saddle points corresponding to a mode with one or more imaginary frequencies associated with the movement of Ng atom, which takes the Ng atom to the B position. On the other hand, in all cases the systems with Ng situated in front of B position correspond to the minimum energy structures. $\text{Kr}@CB[6]$ with Kr at both the positions are at minima on the PES but the isomer with Ng at B

position is 0.5 kcal/mol (ZPE corrected) more stable than that at the A position. Though the energy difference is only 0.5 kcal/mol and in experimental situation Kr at both the positions might be viable, we here continue with the lower energy isomer. We also exclude He trapped analogues since in several attempts we cannot get them as minimum energy structures and the interaction energy is also very low (~ -0.8 kcal/mol).⁹⁰

In CB[6], there are six B positions. In Ne₂@CB[6], two Ne reside at two B positions keeping one B position in between them as vacant. However, in Ar₂@CB[6] and Kr₂@CB[6], two Ng atoms prefer to stay as far apart as possible. They reside at two B positions by keeping two B positions vacant in between. This is due to the lower size of Ne, which does not cause any severe inter-nuclear repulsion even at such a closer Ne-Ne distance. Unlike other cases, such arrangement of Ne inside CB[6] makes it possible to include third Ne atom inside this. On the other hand, incorporation of third Ar or Kr atom inside the CB[6] results in a strong inter-nuclear repulsion making the process unfavorable. In fact, during free optimization, Ar₃ and Kr₃ moieties flip and tend to go out along the open faces of CB[6].

The diameter inside the cavity of CB[6] is measured in two directions, x and y. In one direction, the distance between the middle of C-C bond of $-C_4H_2N_4O_2-$ moiety in two opposite sides is computed and in the other direction, the distance between the middle of the bonds connecting two C atoms of two methylene linkages in two opposite sides is calculated (see structure **1** and Figure 1). Except for Ar₂ and Kr₂ entrapped analogues, in all other cases the change in the diameter caused by the Ng inclusion is quite small ($\leq 0.14 \text{ \AA}$). However, for Ar₂@CB[6] and Kr₂@CB[6], the diameter increases along the Ng-Ng direction by 0.57-0.82 \AA and it contracts along the perpendicular direction of Ng-Ng by 0.48-0.75 \AA .

The preparation energies (ΔE_{prep}), interaction energies (ΔE), dissociation energies (D), dissociation enthalpy values (ΔH) and the NPA charges at Ng center (q_{Ng}) are provided in Table 1. ΔE_{prep} is the energy required for a fragment to acquire the geometry as in the supermolecular complexes from its equilibrium geometry. In accommodating the first Ng atom, the distortion in the shape of CB[6] is very negligible as indicated by the very low ΔE_{prep} value (~ 0.1 kcal/mol). The second and third Ne encapsulations also do not lead to much distortion in the shape of their host. The cavity within the

equilibrium geometry of CB[6] appears to be enough to accommodate them. However, for the second Ar and Kr encapsulations, significant distortion is needed to provide them adequate space. Energies of 1.1 and 2.8 kcal/mol should be paid to reorient the shape of CB[6] in hosting the second Ar and Kr atoms, respectively. In fact, to reduce the bond distances of Ar₂ and Kr₂ from their equilibrium values of 4.115 and 4.310 Å to 3.228 and 3.353 Å, respectively, 1.3 kcal/mol of energy for Ar₂ and 2.3 kcal/mol of energy for Kr₂ would be needed. On the other hand, Ne₂ and Ne₃ do not need any such compression.

ΔE represents the energy difference between the supercomplex and the interacting fragments having the same geometries as those in the supercomplex. In Ne_n@CB[6] cases, the first Ne atom interacts with CB[6] by a stabilizing energy of -4.3 kcal/mol. Even for the second and third Ne atoms, ΔE value per Ne atom does not get reduced. The total ΔE value only gets multiplied with the number of interacting Ne atoms signifying equal acceptability for all the three Ne atoms by the host. In contrast, for Ar and Kr cases, the second Ng atom is somewhat less acceptable compared to the first one. While ΔE values for first Ar and Kr are -4.7 and -7.4 kcal/mol, respectively, ΔE values for Ng₂ encapsulated complexes are -8.3 kcal/mol for Ar₂ and -12.3 kcal/mol for Kr₂.

D values, which represent the energy required to free the trapped Ng atoms from Ng_n@CB[6] resulting in free Ng and CB[6], also describe the stability of these Ng trapped systems. We have computed both, zero point energy (ZPE) uncorrected and corrected dissociation energy values (D_e and D₀, respectively). For Ne_n@CB[6] and Ng@CB[6], due to negligible ΔE_{prep} values, D_e values are almost same in magnitude with ΔE per Ng atom. However, for Ar₂ and Kr₂ encapsulated analogues, D_e values corresponding to the process Ng₂@CB[6] → Ng + Ng@CB[6] are quite low, being 1.5 kcal/mol for Ar₂ and 0.2 kcal/mol for Kr₂ cases. ZPE correction diminishes D_e values to some extent. In fact, for Kr₂, D₀ value becomes negative (-0.5 kcal/mol) implying the instability of Kr₂@CB[6] system. D₀ value ranges within 3.4 to 4.1 kcal/mol for Ne_n@CB[6] systems whereas it is 4.1 kcal/mol for Ar and 6.3 kcal/mol for Kr cases. For the case of the second Ar atom, it becomes 1.0 kcal/mol. ΔH values are positive for all cases showing the endothermic nature of the dissociation processes. However, it is very low for the second Ar case and it is zero for the second Kr case, being well complemented with their D values. ΔH values are within 4.0-4.3 kcal/mol for

Ne_n@CB[6] systems whereas it is slightly higher for Ar (5.1 kcal/mol) and Kr (6.8 kcal/mol) cases. For Ng@CB[6], the endothermicity of the dissociation process gradually increases along Ne to Kr.

The free energy change values (ΔG) for the dissociation processes of Ng_n@CB[6] computed at two different temperatures are provided in Table 2. At room temperature, except for Kr@CB[6], the dissociations of all other Ng encapsulated systems are exergonic in nature. Note that for the dissociation process ΔS is a favorable term. Therefore, to make $T\Delta S$ term less important, we have also checked the viability of these systems at low temperature (77 K). At this temperature, except for the dissociation of the second Ar and Kr atoms form the respective Ng₂@CB[6], all other dissociations are endergonic in nature. On the other hand, the ΔG values at 77 K for the dissociation process following all Ng atoms coming out together from Ng_n@CB[6], i.e., for Ng_n@CB[6] \rightarrow nNg + CB[6] are all endergonic in nature. It implies that multiple Ng atoms cannot come out from Ng_n@CB[6] together. They must follow sequential way to leave. We have further generated a temperature-pressure phase diagram to highlight the temperature-pressure region in which association and dissociation processes would be thermochemically favorable considering Kr@CB[6] as a case study (see Figure 2). At 298 K and 1 atm pressure, the Kr encapsulation process into CB[6] is thermochemically favorable. At this temperature the dissociation of Kr from Kr@CB[6] needs less than 1 atm pressure. At higher temperature the pressure should be increased to make the dissociation process nonspontaneous. However, the required pressure is not very high. At 400 K, around 20 atm pressure is needed to avoid dissociation. For Ne and Ar encapsulated analogues, at moderately low temperature and high pressure they could remain as stable. It may be noted that Ng_n@C₆₀ and their larger analogues have been treated as the noble gas carrier.⁹¹ However, high pressure and high temperature are needed to encapsulate Ng atoms inside these cages and vigorous heating (> 600° C) under vacuum is needed to release the Ng atoms since the barrier for incorporation or release is about 200 kcal/mol for He@C₆₀.^{43,92} Therefore, these systems could be important as noble gas carrier if one wants to avoid a drastic situation. So, here only a slightly low temperature and high pressure are needed and one can get noble gas back at slightly elevated temperature (say room temperature or slightly more than that). Moreover, we

1
2
3 should mention that we adopted CB[6] as just a case study. The larger members of the
4 cucurbit[n]uril family could even encapsulate larger number of Ng atoms. Further,
5 inverted cucurbit[n]uril,⁹³ cyclodextrins,⁹⁴ calixarenes,⁹⁵ pillararene⁹⁶ have similar type of
6 texture and therefore they could also be interesting hosts to accommodate Ng atoms. It
7 may also be noted that the extended frameworks made by CB[6] called polyrotaxanes,⁹⁷
8 which contain several number of CB[6] pockets, could be able to encapsulate a large
9 number of Ng atoms. Still now, studies were mainly focused on fullerene like carbon or
10 BN cages (both large and small members).⁵⁴⁻⁶² No one considered such systems as
11 possible hosts for Ng atoms before. Our present study is just a beginning along this line.
12
13
14
15
16
17
18

19 A large HOMO-LUMO energy gap^{98,99} of a system generally implies its
20 reluctance towards the acceptance of electron in LUMO and the removal of electron from
21 HOMO. Hence, it reflects the electronic stability of a system. It may be noted that as
22 HOMO-LUMO energy gap of a system is a measure of hardness, the stability is
23 connected with the maximum hardness principle (MHP).¹⁰⁰⁻¹⁰² The HOMO-LUMO
24 energy gap in CB[6] is quite high (10.81 eV) reflecting its high stability. Similar to the
25 bare moiety, the Ng entrapped analogues also maintain high HOMO-LUMO energy gap
26 values ranging within 10.77-10.80 eV (see Table 1).
27
28
29
30
31
32

33 NPA charge computed at each center reveals that N and O centers in Ng_n@CB[6]
34 are negatively charged whereas C and H centers are positively charged. A little amount of
35 electron transfer ($\sim 0.01 e^-$) takes place from Ng atoms to the CB[6] moiety. The Wiberg
36 bond indices (WBI)¹⁰³ for Ng-Ng bond (< 0.005) as well as total WBI values (< 0.03) for
37 Ng atoms are also negligible. Low total WBI values for Ng atoms indicate a van der
38 Waals type of interaction in between Ng and CB[6] moiety.
39
40
41
42
43

44 45 46 Nature of interaction

47 We have performed electron density⁷⁵ and energy decomposition⁷⁶ analyses as
48 well as the analysis of non-covalent interaction (NCI)⁷⁷ indices to check the inference
49 obtained from the low WBI.
50
51

52 Different topological descriptors computed at the bond critical points (BCPs) are
53 tabulated in Table 3. In general, ‘closed-shell type bonding’ is interpreted by a low value
54 of electron density ($\rho(r_c)$) and positive value of Laplacian of electron density ($\nabla^2\rho(r_c)$) at
55
56
57
58
59
60

the BCP. On the other hand, high value of $\rho(r_c)$ and negative value of $\nabla^2\rho(r_c)$ are the indicators of the presence of covalent interaction therein. However, this criterion fails in many examples in representing a covalent bond.^{104-109,75;pp. 312-314} Some other descriptors were also applied to describe a bond. Cremer *et al.*¹¹⁰ proposed that if $\nabla^2\rho(r_c) > 0$ and $H(r_c) < 0$, then the bonding might be considered as of partial covalent type. $H(r_c)$, local electron energy density could be calculated as the sum of local kinetic energy density ($G(r_c)$) and local potential energy density ($V(r_c)$). The molecular graphs generated by Multiwfn software⁸⁵ are displayed in Figure S1 (supporting information). It is found that in $\text{Ne}_n@\text{CB}[6]$, $\text{Ar}_2@\text{CB}[6]$ and $\text{Kr}_2@\text{CB}[6]$ systems, each Ng atom is connected with four nearby N centers through maximum electron density (MED) paths whereas in $\text{Ar}@\text{CB}[6]$ and $\text{Kr}@\text{CB}[6]$ systems, the number of such MED paths is six. In these systems, Ng is connected with four N centers at the near side and with one each of N and C centers in the opposite side through MED paths. In addition, there is always an MED path in between two Ng atoms. Now the different topological descriptors computed at the BCPs of these bond paths reveal that $\rho(r_c)$ is small and, $\nabla^2\rho(r_c)$ and $H(r_c)$ are positive in all cases highlighting the presence of closed-shell type bonding therein. The contour plots of $\nabla^2\rho(r_c)$ showing the situation in Ng-Ng bonds are given in Figure 3. The shapes of the valence orbitals of Ng get slightly deformed in these systems.

A high value of ELF⁷⁸ in between two bonded atoms is an indication of the localized electrons therein. It further implies the existence of covalent bonds. On the other hand, a low value of ELF indicates noncovalent type of bonding. In our cases, the color-filled maps of ELF show that there is almost no electron localization either in between two Ng atoms or in between Ng and cage atoms indicating closed-shell type bonding (see Figure S2 in supporting information).

EDA further gives us the contribution from the Pauli repulsion (ΔE_{pauli}), electrostatic (E_{elstat}), orbital (ΔE_{orb}) and dispersion (ΔE_{disp}) energy terms towards the total interaction energy (ΔE_{total}). Since ω B97X-D functional is not available in the ADF(2013.01) program,⁸⁷ we choose the currently developed SSB-D *meta*GGA functional⁸⁶ having Grimme's dispersion correction, which is reported to be excellent in representing weak π - π stacking and H-bonding. CB[6] and Ng or Ng_n are taken as two fragments in this energy partitioning scheme. The results of the EDA are displayed in

Figure 4. ΔE_{disp} is found to be the largest contributor ranging from 49 to 68% towards the total attraction. ΔE_{elstat} is the second most dominating term in the attraction energy (*ca.* 20-37%) whereas the ΔE_{orb} contributes the least towards the same (*ca.* 9-15%). It may also be noted that the contribution from each of the terms gradually increases in moving from Ne to Kr.

NCI isosurfaces⁸⁸ are very widely used to understand the nature of interaction in different types of systems. Figure 5 shows the NCI isosurfaces between the Ng atoms with the parent CB[6] moiety. A continuous color-coding scheme as implemented in NCIPLOT software⁸⁸ is used in these figures. Here, weak van der Waals interactions are shown with green surfaces, whereas strong attractive H-bond interactions and repulsive steric interactions are visualized by blue and red surfaces, respectively. Therefore, the presence of green surfaces between Ng and CB[6] units indicates the presence of a weak van der Waals type of attractive interaction according to the presently used color-coding scheme. Each Ng atom interacts independently with CB[6] and the attractive interaction increases with the increase in the number of Ng atoms. Moreover, the size of the green surfaces relatively increases on increasing the size of the Ng atoms from Ne to Kr. The maximum attractive interaction is found in case of Kr₂@CB[6].

A better understanding about the interactions present in between Ng_n and CB[6] moieties can be revealed through the plots of s versus sign(λ_2) ρ (see Figure 6 for zoomed view and Figure S3 for normal view). In these plots, the very low-density, low-gradient troughs indicate the presence of weak dispersion interactions. Conversely, the low-gradient troughs appearing in the moderately low positive region indicate the repulsive interaction, like steric crowding. Figures 6 and S3 show the presence of dispersion interaction in between Ng_n and CB[6] units, which appears very close to zero density, with slightly negative sign(λ_2) ρ values around -0.005 au. Inclusion of more Ng atoms causes additional attractive interaction between these two units. This can be seen by looking at the troughs around ρ value of -0.005 a.u. from s versus sign(λ_2) ρ plots for the Ne_n@CB[6] systems (Figure 6). The attractive interaction increases monotonically with an increase in the size of Ng atoms, from Ne to Kr.

Dynamics of the systems

An ab initio molecular dynamics simulation at 298 K is carried out up to 1 ps to provide insight into the kinetic stability and dynamical behavior of these systems.¹¹¹ It may be noted that CB[6] has two open faces and therefore, a large nuclear kinetic energy may force the Ng atoms to leave the cavity. The snapshots of the Ng entrapped systems at the end of the simulation (at 1 ps) are presented in Figure 7. The top view of the snapshots is provided in Figure S4 (supporting information). Throughout the simulation, the Ne and Ar atoms in Ng@CB[6] remain within the cavity area of CB[6] and the structural integrity of CB[6] moiety remains essentially the same. The Ng atoms only float within the cage and the cage suffers slight distortion. In Kr@CB[6], Kr atom gravitates towards the open face of CB[6]. In cases of Ng₂@CB[6] after 1 fs Ng₂ units remain within the cavity but they tend to flip in such a way that Ng₂ may go out through the open faces of CB[6]. It gives us a hint that in longer time simulation they might escape from the cavity. The extent of such flipping after 1 ps is the largest in Kr₂ case. In Ne₃@CB[6], after 1 ps one Ne atom almost comes near the oxygen ends situated at the open face whereas other two Ne atoms remain inside the cavity. Note that such type of entropy loss processes often occur at low temperature. Therefore, at lower temperature, due to lower nuclear kinetic energy, Ng atoms might stay within the cavity of CB[6] for longer time. To prove this, we have further performed molecular dynamics simulation at 77 K up to 1 ps time. All the Ng atoms in Ng_n@CB[6] are found to stay well inside the cavity of CB[6] throughout the simulation. The final structures of the simulation after 1 ps time are displayed in Figure 8 (for top view see Figure S5 in supporting information).

Time evolution of energies of these systems is provided in Figure S6 (supporting information). Oscillations in the energy curves are found in all cases. This is due to the movement of Ng atoms, which causes the distortion in the CB[6] moiety producing a somewhat higher energy structure. Such oscillations in energy curve considerably get reduced at lower temperature (77 K) (see Figure S7 in supporting information).

Summary and conclusions

We have performed both electronic structure calculations and ab initio molecular dynamics study to assess the efficacy of CB[6] to be a host for Ng atoms. CB[6] is found to encapsulate three Ne atoms having D₀ values within the range of 3.4-4.1 kcal/mol. On

the other hand, it can afford space for maximum two Ar or Kr atoms, due to their larger radii. For the first Ar and Kr cases, D_0 values are 4.1 and 6.9 kcal/mol, respectively. But for the second cases, D_0 values decrease drastically. It even becomes negative (-0.5 kcal/mol) in the Kr_2 case implying the instability of this system. All the Ng dissociations from $\text{Ng}_n@\text{CB}[6]$ are endothermic in nature. The dissociations even become more endothermic in moving from Ne to Kr entrapped analogues. At room temperature, except for $\text{Kr}@\text{CB}[6]$, all other dissociation processes are found to be exergonic in nature. However, they turn out to be endergonic at low temperature. The temperature-pressure phase diagram for $\text{Kr}@\text{CB}[6]$ shows that the temperature-pressure regions can be demarcated where association and dissociation processes would be thermochemically favorable. The association and dissociation processes associated with CB[6] at ambient temperature and pressure suggest that it may be used as a safe and potential Ng carrier as it can avoid any drastic situation as needed in case of $\text{Ng}_n@\text{C}_{60}$.^{43,92}

CB[6] faces negligible distortion in accommodating Ne_n , Ar and Kr; however, for the encapsulation of second Ar or Kr, it suffers considerable distortion, being larger in the latter case. Similar to the CB[6], Ng encapsulated analogues maintain high HOMO-LUMO gap values showing their electronic stability. Nature of interaction between Ng atoms and CB[6] is understood through the analyses of WBI and NCI indices as well as from the electron density and energy decomposition analyses. Low WBI suggests a closed-shell type of bonding between Ng and CB[6]. Molecular graphs obtained from the electron density analysis show that except for $\text{Ar}_2@\text{CB}[6]$ and $\text{Kr}_2@\text{CB}[6]$, there are four MED paths in between each Ng atom and its nearby N centers in CB[6]. In $\text{Ar}_2@\text{CB}[6]$ and $\text{Kr}_2@\text{CB}[6]$, the number of MED paths is six. Two Ng atoms in $\text{Ng}_n@\text{CB}[6]$ are also connected through an MED path. Different topological descriptors reveal that the interactions between two Ng atoms or between an Ng atom and N centers are of non-covalent type. EDA shows that ΔE_{disp} is the predominant attraction term (*ca.* 49-68%) during the interactions between Ng and CB[6]. The presence of green surfaces between Ng and CB[6] units in NCI isosurface plots further reflects the presence of van der Waals type of attractive interaction therein.

An ab initio molecular dynamics simulation at 298 K shows that Ne and Ar atoms in $\text{Ng}@\text{CB}[6]$ remain within the cavity area of CB[6] up to 1 ps. However, the Kr atom

in Kr@CB[6] tries to almost go out of the cavity. For Ng₂@CB[6], they approach towards the open faces of CB[6], although Ng₂ units stay inside CB[6] up to 1 ps. In Ne₃@CB[6], one Ne atom almost reaches near the oxygen ends situated at the upper side of the open face after 1 ps. However, they might be stable at lower temperature as the molecular dynamics simulation at 77 K shows that all the Ng atoms in Ng_n@CB[6] stay well inside the cavity of CB[6].

Acknowledgements

PKC would like to thank DST, New Delhi for the J. C. Bose National Fellowship. SP thanks CSIR, New Delhi and SM thanks UGC, New Delhi for their fellowships.

References

1. Behrend, R.; Meyer, E.; Rusche, F. Ueber Condensationsprodukte aus Glycoluril und Formaldehyd. *Eur. J. Org. Chem.*, **1905**, 339, 1–37.
2. Freeman, W. A.; Mock, W. L.; Shih, N.-Y. Cucurbituril. *J. Am. Chem. Soc.*, **1981**, 103, 7367–7368.
3. Lee, J. W.; Samal, S.; Selvapalam, N.; Kim, H.-J.; Kim, K. Cucurbituril Homologues and Derivatives: New Opportunities in Supramolecular Chemistry. *Acc. Chem. Res.*, **2003**, 36, 621–630.
4. Liu, Y.; Han, B.-H.; Chen, Y.-T. Molecular Recognition and Complexation Thermodynamics of Dye Guest Molecules by Modified Cyclodextrins and Calixarenesulfonates. *J. Phys. Chem. B*, **2002**, 106, 4678–4687.
5. Lagona, J.; Mukhopadhyay, P.; Chakrabarti, S.; Isaacs, L. The Cucurbit[n]uril Family. *Angew. Chem. Int. Ed.*, **2005**, 44, 4844–4870.
6. Buschmann, H.-J.; Schollmeyer, E. Cucurbituril and β -Cyclodextrin as Hosts for the Complexation of Organic Dyes. *J. Incl. Phenom. Mol. Recog. Chem.*, **1997**, 29, 167–174.
7. Moon, K.; Kaifer, A. E. Modes of Binding Interaction between Viologen Guests and the Cucurbit[7]uril Host. *Org. Lett.*, **2004**, 6, 185–188.
8. Whang, D.; Heo, J.; Park, J. H.; Kim, K. A Molecular Bowl with Metal Ion as Bottom: Reversible Inclusion of Organic Molecules in Cesium Ion Complexed Cucurbituril. *Angew. Chem. Int. Ed.*, **1998**, 37, 78–80.
9. Buschmann, H.-J.; Jansen, K.; Meschke, C.; Schollmeyer, E. Thermodynamic Data for Complex Formation Between Cucurbituril and Alkali and Alkaline Earth Cations in Aqueous Formic Acid Solution. *J. Solution Chem.*, **1998**, 27, 135–140.
10. Marquez, C.; Hudgins, R. R.; Nau, W. M. Mechanism of Host–Guest Complexation by Cucurbituril. *J. Am. Chem. Soc.*, **2004**, 126, 5806–5816.
11. Mock, W. L.; Pierpont, J. A Cucurbituril-based Molecular Switch. *J. Chem. Soc., Chem. Commun.*, **1990**, 1509–1511.

- 1
2
3
4
5
6
7
8
9
10
11
12
13
14
15
16
17
18
19
20
21
22
23
24
25
26
27
28
29
30
31
32
33
34
35
36
37
38
39
40
41
42
43
44
45
46
47
48
49
50
51
52
53
54
55
56
57
58
59
60
12. Day, A. I.; Blanch, R. J.; Arnold, A. P.; Lorenzo, S.; Lewis, G. R.; Dance, I. A Cucurbituril-Based Gyrosane: A New Supramolecular Form. *Angew. Chem. Int. Ed.*, **2002**, *41*, 275–277.
 13. Pan, S.; Mondal, S.; Chattaraj, P. K. Cucurbiturils as Promising Hydrogen Storage Materials: A Case Study of Cucurbit[7]uril. *New J. Chem.*, **2013**, *37*, 2492–2499.
 14. Lim, S.; Kim, H.; Selvapalam, N.; Kim, K. J.; Cho, S. J.; Seo, G.; Kim, K. Cucurbit[6]uril: Organic Molecular Porous Material with Permanent Porosity, Exceptional Stability, and Acetylene Sorption Properties. *Angew. Chem., Int. Ed.*, **2008**, *47*, 3352–3355.
 15. Kim, H.; Kim, Y.; Yoon, M.; Lim, S.; Park, S. M.; Seo, G.; Kim, K. Highly Selective Carbon Dioxide Sorption in an Organic Molecular Porous Material. *J. Am. Chem. Soc.*, **2010**, *132*, 12200–12202.
 16. Tian, J.; Ma, S.; Thallapally, P. K.; Fowler, D.; McGrail, B. P.; Atwood, J. L. Cucurbit[7]uril: An Amorphous Molecular Material for Highly Selective Carbon dioxide Uptake. *Chem. Commun.*, **2011**, *47*, 7626–7628.
 17. Khriachtchev, L.; Tanskanen, H.; Cohen, A.; Gerber, R. B.; Lundell, J.; Pettersson, M.; Kiljunen, H.; Räsänen, M. A Gate to Organokrypton Chemistry: HKrCCH. *J. Am. Chem. Soc.*, **2003**, *125*, 6876–6877.
 18. Tanskanen, H.; Khriachtchev, L.; Lundell, J.; Kiljunen, H.; Räsänen, M. Chemical Compounds Formed from Diacetylene and Rare-Gas Atoms: HKrC₄H and HXeC₄H. *J. Am. Chem. Soc.*, **2003**, *125*, 16361–16366.
 19. Feldman, V. I.; Sukhov, F. F. Formation and Decay of Transient Xenon dihydride resulting from Hydrocarbon Radiolysis in a Xenon Matrix. *Chem. Phys. Lett.*, **1996**, *225*, 425–430.
 20. Feldman, V. I.; Sukhov, F. F.; Orlov, A. Y. Further Evidence for Formation of Xenon dihydride from Neutral Hydrogen atoms: A comparison of ESR and IR Spectroscopic Results. *Chem. Phys. Lett.*, **1997**, *280*, 507–512.
 21. Thompson, C. A.; Andrews, L. Noble Gas Complexes with BeO: Infrared Spectra of NG-BeO (NG = Ar, Kr, Xe). *J. Am. Chem. Soc.*, **1994**, *116*, 423–424.
 22. Thompson, C. A.; Andrews, L. Reactions of Laser Ablated Be Atoms with O₂: Infrared Spectra of Beryllium Oxides in Solid Argon. *J. Chem. Phys.*, **1994**, *100*, 8689–8699.
 23. Cooke, S. A.; Gerry, M. C. L. XeAuF. *J. Am. Chem. Soc.*, **2004**, *126*, 17000–17008.
 24. Michaud, M.; Gerry, M. C. L. XeCu Covalent Bonding in XeCuF and XeCuCl, Characterized by Fourier Transform Microwave Spectroscopy Supported by Quantum Chemical Calculations. *J. Am. Chem. Soc.*, **2006**, *128*, 7613–7621.
 25. Jiménez-Halla, C. Ó.; Fernández, I.; Frenking, G. Is it Possible to Synthesize a Neutral Noble Gas Compound Containing a Ng-Ng Bond? A Theoretical Study of H-Ng-Ng-F (Ng=Ar, Kr, Xe). *Angew. Chem. Int. Ed.*, **2009**, *48*, 366–369.
 26. Fernández, I.; Frenking, G. Neutral Noble Gas Compounds Exhibiting a Xe-Xe Bond: Structure, Stability and Bonding Situation. *Phys. Chem. Chem. Phys.*, **2012**, *14*, 14869–14877.
 27. Pan, S.; Contreras, M.; Romero, J.; Reyes, A.; Merino, G.; Chattaraj, P. K. C₅Li₇⁺ and O₂Li₅⁺ as Noble Gas Trapping Agents. *Chem. Eur. J.*, **2013**, *19*, 2322–2329.
 28. Pan, S.; Jalife, S.; Kumar, M.; Subramanian, V.; Merino, G.; Chattaraj, P. K. Structure and Stability of (NG)_nCN₃Be₃⁺ Clusters and Comparison with (NG)BeY^{0/+}

- (Ng=Noble Gas and Y=O, S, Se, Te). *ChemPhysChem*, **2013**, *14*, 2511-2517.
29. Pan, S.; Moreno, D.; Cabellos, J. L.; Merino, G.; Chattaraj, P. K. Ab Initio Study on
the Stability of Ng_nBe₂N₂, Ng_nBe₃N₂ and NgBeSiN₂ Clusters. *ChemPhysChem*, **2014**,
15, 2618-2625.
30. Pan, S.; Moreno, D.; Merino, G.; Chattaraj, P. K. Stability of Noble-Gas-Bound SiH₃⁺
Clusters. *ChemPhysChem*, **2014**, *15*, 3554-3564.
31. Pan, S.; Moreno, D.; Cabellos, J. L.; Romero, J.; Reyes, A.; Merino, G.; Chattaraj, P.
K. In Quest of Strong Be–Ng Bonds among the Neutral Ng–Be Complexes. *J. Phys.
Chem. A* **2014**, *118*, 487-494.
32. Pan, S.; Saha, R.; Chattaraj, P. K. Exploring the Nature of Silicon-Noble Gas Bonds
in H₃SiNgNSi and HSiNgNSi Compounds (Ng = Xe, Rn). *Int. J. Mol. Sci.*, **2015**, *16*,
6402-6418.
33. Chakraborty, D.; Chattaraj, P. K. In Quest of a Superhalogen Supported Covalent
Bond Involving a Noble Gas Atom. *J. Phys. Chem. A*, **2015**, *119*, 3064-3074.
34. Lundell, J.; Cohen, A.; Gerber, R. B. Quantum Chemical Calculations on Novel
Molecules from Xenon Insertion into Hydrocarbons. *J. Phys. Chem. A*, **2002**, *106*,
11950-11955.
35. Pan, S.; Jalife, S.; Romero, J.; Reyes, A.; Merino, G.; Chattaraj, P. K. Attractive Xe–
Li interaction in Li-decorated clusters. *Comput. Theor. Chem.*, **2013**, *1021*, 62-69.
36. Lockyear, J. F.; Douglas, K.; Price, S. D.; Karwowska, M.; Fijałkowski, K. J.;
Grochala, W.; Remeš, M.; Roithová, J.; Schröder, D. Generation of the ArCF₂²⁺
Dication. *J. Phys. Chem. Lett.*, **2010**, *1*, 358-362.
37. Grochala, W. A Metastable He–O Bond inside a Ferroelectric Molecular Cavity:
(HeO)(LiF)₂. *Phys. Chem. Chem. Phys.*, **2012**, *14*, 14860-14868.
38. Antoniotti, P.; Bottizzo, E.; Operti, L.; Rabezzana, R.; Borocci, S.; Grandinetti, F.
F₃Ge-Xe⁺: A Xenon-Germanium Molecular Species. *J. Phys. Chem. Lett.*, **2010**, *1*,
2006-2010.
39. Operti, L.; Rabezzana, R.; Turco, F.; Borocci, S.; Giordani, M.; Grandinetti, F.
Xenon–Nitrogen Chemistry: Gas-Phase Generation and Theoretical Investigation of
the Xenon–Difluoronitrenium Ion F₂N-Xe⁺. *Chem. Eur. J.*, **2011**, *17*, 10682-10689.
40. Sirohiwal, A.; Manna, D.; Ghosh, A.; Jayasekharan, T.; Ghanty, T. K. Theoretical
prediction of rare gas containing hydride cations: HRgBF⁺ (Rg = He, Ar, Kr, and Xe).
J. Phys. Chem. A, **2013**, *117*, 10772-10782.
41. Manna, D.; Ghosh, A.; Ghanty, T. K. Theoretical prediction of XRgCO⁺ ions (X = F,
Cl, and Rg = Ar, Kr, Xe), *J. Phys. Chem. A*, **2013**, *117*, 14282-14292.
42. Saunders, M.; Jiménez-Vázquez, H. A.; Cross, R. J.; Poreda, R. J. Stable Compounds
of Helium and Neon: He@C₆₀ and Ne@C₆₀. *Science*, **1993**, *259*, 1428–1430.
43. Saunders, M.; Jiménez-Vázquez, H. A.; Cross, R. J. Incorporation of Helium, Neon,
Argon, Krypton, and Xenon into Fullerenes using High Pressure. *J. Am. Chem. Soc.*,
1994, *116*, 2193-2194.
44. Bühl, M.; Patchkovskii, S.; Thiel, W. Interaction energies and NMR chemical shifts
of noble gases in C₆₀. *Chem. Phys. Lett.*, **1997**, *275*, 14–18.
45. Syamala, M. S.; Cross, R. J.; Saunders, M. ¹²⁹Xe NMR Spectrum of Xenon Inside
C₆₀. *J. Am. Chem. Soc.*, **2002**, *124*, 6216–6219.
46. Cross, R. J.; Khong, A.; Saunders, M. Using Cyanide To Put Noble Gases inside C₆₀.
J. Org. Chem., **2003**, *68*, 8281–8283.

- 1
2
3 47. Peres, T.; Cao, B. P.; Cui, W. D.; Khong, A.; Cross, R. J.; Saunders, M.; Lifshitz, C.
4 Some New Diatomic Molecule Containing Endohedral Fullerenes. *Int. J. Mass*
5 *Spectrom.*, **2001**, *210*, 241–247.
6
7 48. Khong, A.; Jimenez-Vazquez, H. A.; Saunders, M.; Cross, R. J.; Laskin, J.; Peres, T.;
8 Lifshitz, C.; Strongin, R.; Smith, A. B. An NMR Study of He₂ Inside C₇₀. *J. Am.*
9 *Chem. Soc.*, **1998**, *120*, 6380–6383.
10
11 49. Laskin, J.; Peres, T.; Lifshitz, C.; Saunders, M.; Cross, R. J.; Khong, A. An Artificial
12 Molecule of Ne₂ inside C₇₀. *Chem. Phys. Lett.*, **1998**, *285*, 7–9.
13
14 50. Sternfeld, T.; Hoffman, R. E.; Saunders, M.; Cross, R. J.; Syamala, M. S.; Rabinovitz,
15 M. Two Helium Atoms inside Fullerenes: Probing the Internal Magnetic Field in
16 C₆₀⁶⁻ and C₇₀⁶⁻. *J. Am. Chem. Soc.*, **2002**, *124*, 8786–8787.
17
18 51. Patchkovskii, S.; Thiel, W. Equilibrium Yield for Helium Incorporation into
19 Buckminsterfullerene: Quantum-chemical Evaluation. *J. Chem. Phys.*, **1997**, *106*,
1796–1799.
20
21 52. Khatua, M.; Pan, S.; Chattaraj, P. K. Movement of Ng₂ Molecules Confined in a C₆₀
22 Cage: An ab initio Molecular Dynamics Study. *Chem. Phys. Lett.*, **2014**, *610-611*,
351–356.
23
24 53. Weiske, T.; Bohme, D. K.; Schwartz, H. Injection of Helium Atoms in to Doubly and
25 Triply Charged C₆₀ Cations. *J. Phys. Chem.*, **1991**, *95*, 8451–8452.
26
27 54. Jiménez-Vázquez, H. A.; Tamariz, J.; Cross, R. J. Binding Energy in and Equilibrium
28 Constant of Formation for the Dodecahedrane compounds He@C₂₀H₂₀ and
Ne@C₂₀H₂₀. *J. Phys. Chem. A*, **2001**, *105*, 1315–1319.
29
30 55. Haaland, A.; Shorokhov, D. J.; Tverdova, N. V. Topological Analysis of Electron
31 Densities: Is the Presence of an Atomic Interaction Line in an Equilibrium Geometry
32 a Sufficient Condition for the Existence of a Chemical Bond? *Chem. Eur. J.*, **2004**,
10, 4416–4421.
33
34 56. Strenalyuk, T.; Haaland, A. Chemical Bonding in the Inclusion Complex of He in
35 Adamantane (He@adam): The Origin of the Barrier to Dissociation. *Chem. Eur. J.*,
36 **2008**, *14*, 10223–10226.
37
38 57. von Hopffgarten, M.; Frenking, G. Chemical Bonding in the Inclusion Complex of
39 He in Adamantane, He@adam: Antithesis and Complement. *Chem. Eur. J.*, **2008**, *14*,
40 10227–10231.
41
42 58. Moran, D.; Woodcock, H. L.; Chen, Z. F.; Schaefer, H. F.; Schleyer, P. v. R. On the
43 Viability of Small Endohedral Hydrocarbon Cage Complexes: X@C₄H₄, X@C₈H₈,
44 X@C₈H₁₄, X@C₁₀H₁₆, X@C₁₂H₁₂, and X@C₁₆H₁₆. *J. Am. Chem. Soc.*, **2003**, *125*,
45 11442–11451.
46
47 59. Zou, W.; Liu, Y.; Liu, W.; Wang, T.; Boggs, J. E. He@Mo₆Cl₈F₆: A Stable Complex
48 of Helium. *J. Phys. Chem. A*, **2010**, *114*, 646–651.
49
50 60. Khatua, M.; Pan, S.; Chattaraj, P. K. Confinement Induced Binding of Noble Gas
atoms. *J. Chem. Phys.*, **2014**, *140*, 164306.
51
52 61. Cross, R. J.; Saunders, M.; Prinzbach, H. Putting Helium inside Dodecahedrane. *Org.*
53 *Lett.*, **1999**, *1*, 1479–1481.
54
55 62. Darzynkiewicz, R. B.; Scuseria, G. E. Noble Gas Endohedral Complexes of C₆₀
Buckminsterfullerene. *J. Phys. Chem. A*, **1997**, *101*, 7141–7144.
56
57 63. Krapp, A.; Frenking, G. Is This a Chemical Bond? A Theoretical Study of Ng₂@C₆₀
(Ng=He, Ne, Ar, Kr, Xe). *Chem. Eur. J.*, **2007**, *13*, 8256–8270.

- 1
2
3
4
5
6
7
8
9
10
11
12
13
14
15
16
17
18
19
20
21
22
23
24
25
26
27
28
29
30
31
32
33
34
35
36
37
38
39
40
41
42
43
44
45
46
47
48
49
50
51
52
53
54
55
56
57
58
59
60
64. Cerpa, E.; Krapp, A.; Flores-Moreno, R.; Donald, K. J.; Merino, G. Influence of Endohedral Confinement on the Electronic Interaction between He atoms: A $\text{He}_2@\text{C}_{20}\text{H}_{20}$ Case Study. *Chem. Eur. J.*, **2009**, *15*, 1985–1990.
 65. Chakraborty, D.; Chattaraj, P. K. Confinement Induced Binding in Noble Gas atoms within a BN-doped Carbon Nanotube. *Chem. Phys. Lett.*, **2015**, *621*, 29–34.
 66. Berbeci, L. S.; Wang, W.; Kaifer, A. E. Drastically Decreased Reactivity of Thiols and Disulfides Complexed by Cucurbit[6]uril. *Org. Lett.*, **2008**, *10*, 3721–3724.
 67. Buschmann, H.-J.; Jansen, K.; Schollmeyer, E. The Formation of Cucurbituril Complexes with Amino Acids and Amino Alcohols in Aqueous Formic acid Studied by Calorimetric Titrations. *Thermochim. Acta*, **1998**, *317*, 95–98.
 68. Buschmann, H.-J.; Meschke, C.; Schollmeyer, E. Formation of Pseudorotaxanes between Cucurbituril and some 4,4'-bipyridine Derivatives. *An. Quim. Int. Ed.*, **1998**, *94*, 241–243.
 69. Buschmann, H.-J.; Jansen, K.; Schollmeyer, E. Cucurbituril as Host Molecule for the Complexation of Aliphatic Alcohols, Acids and Nitriles in Aqueous Solution. *Thermochim. Acta*, **2000**, *346*, 33–36.
 70. Jansen, K.; Wego, A.; Buschmann, H.-J.; Schollmeyer, E. Einfluß von Salzen und Huminstoffen auf die Komplexbildung von Aromaten mit dem makrocyclischen Liganden Cucurbituril. *Vom Wasser*, **2000**, *94*, 177–190.
 71. Jansen, K.; Wego, A.; Buschmann, H.-J.; Schollmeyer, E. H-NMR-Untersuchungen der Komplexbildung von aromatischen Aminen und Cucurbituril in wässrigen Lösungen. *Vom Wasser*, **2000**, *95*, 229–236.
 72. Buschmann, H.-J.; Jansen, K.; Schollmeyer, E. Cucurbituril and α - and β -Cyclodextrins as Ligands for the Complexation of Nonionic Surfactants and Polyethyleneglycols in Aqueous Solutions. *J. Inclusion Phenom. Macrocyclic Chem.*, **2000**, *37*, 231–236.
 73. Sundararajan, M.; Solomon, R. V.; Ghosh, S. K.; Venuvanalingam, P. Elucidating the Structures and Binding of Halide Ions bound to Cucurbit[6]uril, Hemi-cucurbit[6]uril and Bambus[6]uril using DFT Calculations. *RSC Adv.*, **2011**, *1*, 1333–1341.
 74. Sundararajan, M.; Ghosh, S. K. Elucidating the Mechanism of Binding of Chromate to Cucurbit[6]uril: A DFT Study. *J. Incl. Phenom. Macrocycl. Chem.*, **2012**, *72*, 437–441.
 75. Bader, R. F. W. *Atoms in Molecules: A Quantum Theory*; Oxford University Press: Oxford, **1990**.
 76. a) Morokuma, K. Why do molecules interact? The origin of Electron Donor-Acceptor Complexes, Hydrogen bonding and Proton affinity. *Acc. Chem. Res.*, **1977**, *10*, 294–300; b) Ziegler, T.; Rauk, A. On the Calculation of bonding Energies by the Hartree Fock Slater Method. *Theor. Chim. Acta*, **1977**, *46*, 1–10; c) Ziegler, T.; Rauk, A.; Baerends, E. J. On the Calculation of Multiplet Energies by the Hartree-Fock-Slater Method. *Theor. Chim. Acta*, **1977**, *43*, 261–271; d) von Hopffgarten, M.; G. Frenking, Energy Decomposition Analysis. *Wiley Interdiscip. Rev. Comput. Mol. Sci.*, **2012**, *2*, 43–62.
 77. Johnson, E. R.; Keinan, S.; Mori-Sánchez, P.; Contreras-García, J.; Cohen, A. J.; Yang, W. Revealing Noncovalent Interactions. *J. Am. Chem. Soc.*, **2010**, *132*, 6498–6506.
 78. Becke, A. D.; Edgecombe, K. E. A Simple Measure of Electron Localization in

- 1
2
3 Atomic and Molecular Systems. *J. Chem. Phys.*, **1990**, *92*: 5397–5403.
4
5 79. Marx, D.; Hutter, J. In Proceedings of Modern Methods and Algorithms of Quantum
6 Chemistry, Grotendorst, J.; Ed.; John von Neumann Institute for Computing: (Jurich,
7 Germany, **2000**).
8
9 80. Schlegel, H. B.; Millam, J. M.; Iyengar, S. S.; Voth, G. A.; Daniels, A. D.; Scuseria,
10 G. E.; Frisch, M. J. Ab Initio Molecular Dynamics: Propagating the Density Matrix
11 with Gaussian Orbitals. *J. Chem. Phys.*, **2001**, *114*, 9758–9763.
12
13 81. Iyengar, S. S.; Schlegel, H. B.; Millam, J. M.; Voth, G. A.; Scuseria, G. E.; Frisch,
14 M. J. Ab Initio Molecular Dynamics: Propagating the Density Matrix with Gaussian
15 Orbitals. II. Generalization based on Mass-weighting, Idempotency, Energy
16 Conservation, and Choice of Initial Conditions. *J. Chem. Phys.*, **2001**, *115*, 10291–
17 10302.
18
19 82. Schlegel, H. B.; Iyengar, S. S.; Li, X.; Millam, J. M.; Voth, G. A.; Scuseria, G. E.;
20 Frisch, M. J. Ab Initio Molecular Dynamics: Propagating the Density Matrix with
21 Gaussian Orbitals. III. Comparison with Born-Oppenheimer Dynamics. *J. Chem.*
22 *Phys.*, **2002**, *117*, 8694–8704.
23
24 83. Chaim J.-D.; Head-Gordon, M. Long-range Corrected Hybrid Density Functionals
25 with Damped Atom–Atom Dispersion Corrections. *Phys. Chem. Chem. Phys.*, **2008**,
26 *10*, 6615–6620.
27
28 84. Frisch, M. J. *et al.*, Gaussian 09, Revision C.01, Gaussian, Inc., Wallingford CT,
29 **2010**.
30
31 85. Lu, T.; Chen, F. W. Multiwfn: A Multifunctional Wavefunction Analyzer. *J. Comput.*
32 *Chem.*, **2012**, *33*, 580–592.
33
34 86. Swart, M.; Solà, M.; Bickelhaupt, F. M. A new All-round Density Functional based
35 on Spin states and S_N^2 Barriers. *J. Chem. Phys.*, **2009**, *131*, 094103–09411.
36
37 87. ADF2013.01, Baerends, E. J. *et al.* SCM, Theoretical Chemistry, Vrije Universiteit,
38 Amsterdam, The Netherlands, **2013**.
39
40 88. Contreras-Garcia, J.; Johnson, E. R.; Keinan, S.; Chaudret, R. ; Piquemal, J.-P.;
41 Beratan, D. N.; Yang, W. NCIPILOT: A Program for Plotting Non-covalent
42 Interaction Regions. *J. Chem. Theory Comput.*, **2011**, *7*, 625–632.
43
44 89. We have also tried the possibility of Ng to be situated outside the cavity. Free
45 optimizations are carried out putting Ng atoms at outside of the open face interacting
46 with O centers. During free optimizations Ar and Kr atoms go down to the cavity of
47 CB[6] whereas Ne could stay there interacting with a couple of O centers but the
48 dissociation energy is found to be only 0.8 kcal/mol.
49
50 90. We have attempted several times to make the structures as NIMAG = 0 by following
51 the mode of the imaginary frequency but every time we got structures having one or
52 more imaginary frequency(ies). The small imaginary frequency may arise form the
53 tiny maxima on the potential energy surface. However, for each structure the total
54 energy changes very little. Each time we obtained interaction energy as around -0.8
55 kcal/mol per He atom whereas ZPE corrected dissociation energy is around 0.5
56 kcal/mol per He atom. Since the size of the He is very low, the stabilizing dispersion
57 contribution is also low. This is the reason of getting very small interaction energy.
58
59 91. Becker, L.; Poreda, R. J.; Bunch, T. E. Fullerenes: An extraterrestrial
60 Carbon Carrier Phase for Noble Gases. *Proc. Natl. Acad. Sci. U.S.A.*, **2000**, *97*, 2979–
2983.

- 1
2
3 92. Patchkovskii, S.; Thiel, W. How does Helium Get into Buckminsterfullerene? *J. Am.
4 Chem. Soc.*, **1996**, *118*, 7164-7172.
5
6 93. Isaacs, L.; Park, S.-K.; Liu, S.; Ko, Y. H.; Selvapalam, N.; Kim, Y.; Kim, H.; Zavalij,
7 P. Y.; Kim, G.-H.; Lee, H.-S.; Kim, K. The Inverted Cucurbit[n]uril Family. *J. Am.
8 Chem. Soc.*, **2005**, *127*, 18000-18001.
9
10 94. Menuel, S.; Joly, J.-P.; Courcot, B.; Elysée, J.; Ghermani, N.-E.; Marsura, A.
11 Synthesis and inclusion ability of a bis- β -cyclodextrin pseudo-cryptand towards
12 Busulfan anticancer agent. *Tetrahedron*, **2007**, *63*, 1706-1714.
13
14 95. McMahon, G.; O'Malley, S.; Nolan, K.; Diamond, D. (2003). Important Calixarene
15 Derivatives – their Synthesis and Applications. *Arkivoc*, **2003**, Part (vii), 23–31.
16
17 96. Ogoshi, T.; Kanai, S.; Fujinami, S.; Yamagishi, T.-a.; Nakamoto, Y., *para*-bridged
18 Symmetrical pillar[5]arenes: Their Lewis acid Catalyzed Synthesis and Host-Guest
19 Property. *J. Am. Chem. Soc.*, **2008**, *130*, 5022–5023.
20
21 97. Kim, K. Mechanically Interlocked Molecules Incorporating Cucurbituril and their
22 Supramolecular Assemblies. *Chem. Soc. Rev.*, **2002**, *31*, 96–107.
23
24 98. Manolopoulos, D. E.; May, J. C.; Down, S. E. Theoretical Studies of the Fullerenes:
25 C₃₄ to C₇₀. *Chem. Phys. Lett.*, **1991**, *181*, 105–111.
26
27 99. Aihara, J. Reduced HOMO–LUMO Gap as an Index of Kinetic Stability for
28 Polycyclic Aromatic Hydrocarbons. *J. Phys. Chem. A*, **1999**, *103*, 7487–7495.
29
30 100. Chattaraj, P. K.; Perez, P.; Zevallos, J.; Toro-Labbé, A. Ab initio SCF and DFT
31 Studies on Solvent Effects of Intramolecular Rearrangement Reactions. *J. Phys.
32 Chem. A*, **2001**, *105*, 4272-4283.
33
34 101. Cedillo, A.; Chattaraj, P. K.; Parr, R. G. An Atoms- in- Molecules Partitioning of the
35 Density. *Int. J. Quantum Chem.*, **2000**, *77*, 403-407.
36
37 102. Pan, S.; Solà, M; Chattaraj, P. K. On the Validity of the Maximum Hardness
38 Principle and the Minimum Electrophilicity Principle during Chemical Reactions. *J.
39 Phys. Chem. A*, **2013**, *117*, 1843-1852.
40
41 103. Wiberg, K. B. Application of the Pople-Santry-Segal CNDO method to the
42 Cyclopropylcarbinyl and Cyclobutyl Cation and to Bicyclobutane. *Tetrahedron*,
43 **1968**, *24*, 1083–1096.
44
45 104. Cioslowski, J.; Mixon, S. T. Universality among Topological Properties of Electron
46 Density associated with the Hydrogen–Hydrogen Nonbonding Interactions. *Can. J.
47 Chem.*, **1992**, *70*, 443–449.
48
49 105. Cioslowski, J.; Mixon, S. T. Topological Properties of Electron Density in search of
50 Steric Interactions in Molecules: Electronic Structure Calculations on ortho-
51 substituted Biphenyls. *J. Am. Chem. Soc.*, **1992**, *114*, 4382–4387.
52
53 106. Pan, S.; Gupta, A.; Mandal, S.; Moreno, D.; Merino, G.; Chattaraj, P. K. Metastable
54 Behavior of Noble Gas inserted Tin and Lead Fluorides. *Phys. Chem. Chem. Phys.*
55 **2015**, *17*, 972-982.
56
57 107. Cerpa, E.; Krapp, A.; Vela, A.; Merino, G. The Implications of Symmetry of the
58 External Potential on Bond Paths. *Chem. Eur. J.*, **2008**, *14*, 10232–10234.
59
60 108. Macchi, P.; Proserpio, D. M.; Sironi, A. J. Experimental Electron Density in a
Transition Metal Dimer: Metal–Metal and Metal–Ligand Bonds. *J. Am. Chem. Soc.*,
1998, *120*, 13429–13435.
109. Macchi, P.; Garlaschelli, L.; Martinengo, S.; Sironi, A. J. Charge Density in
Transition Metal Clusters: Supported vs Unsupported Metal-Metal Interactions. *J. Am.*

- 1
2
3 *Chem. Soc.*, **1999**, *121*, 10428–10429.
4
5 110. Cremer, D.; Kraka, E. Chemical Bonds without Bonding Electron Density — Does
6 the Difference Electron-Density Analysis Suffice for a Description of the Chemical
7 Bond? *Angew. Chem., Int. Ed.*, **1984**, *23*, 627–628.
8
9 111. Due to the large volume of the output file generated from the ADMP simulation, we
have restricted our simulation up to 1 ps.
10
11
12
13
14
15
16
17
18
19
20
21
22
23
24
25
26
27
28
29
30
31
32
33
34
35
36
37
38
39
40
41
42
43
44
45
46
47
48
49
50
51
52
53
54
55
56
57
58
59
60

Figures

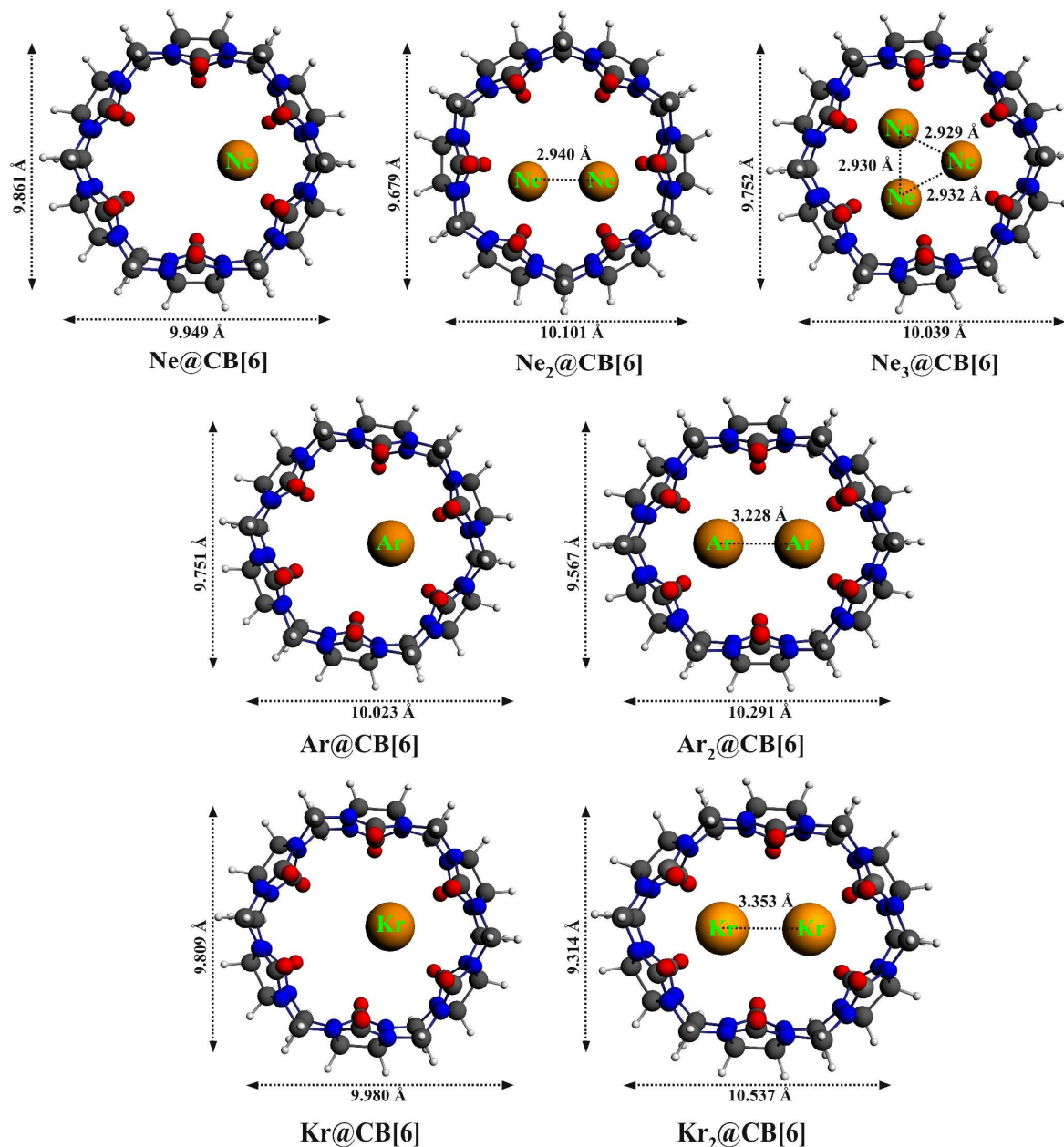


Figure 1. The optimized geometries of $\text{Ng}_n@\text{CB}[6]$ at the $\omega\text{B97X-D}/6-311\text{G}(2\text{d},\text{p})$ level.

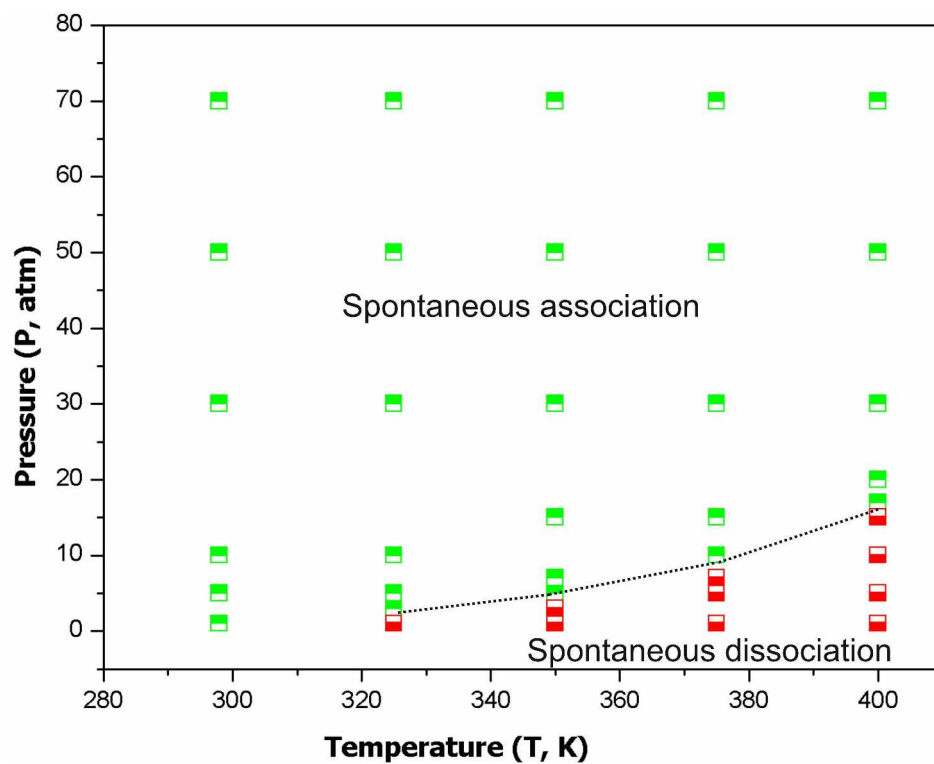


Figure 2. A temperature-pressure phase diagram for the process, $\text{Kr}@\text{CB}[6] \rightarrow \text{Kr} + \text{CB}[6]$ showing the regions with $\Delta G < 0$ (spontaneous dissociation) and $\Delta G > 0$ (spontaneous association).

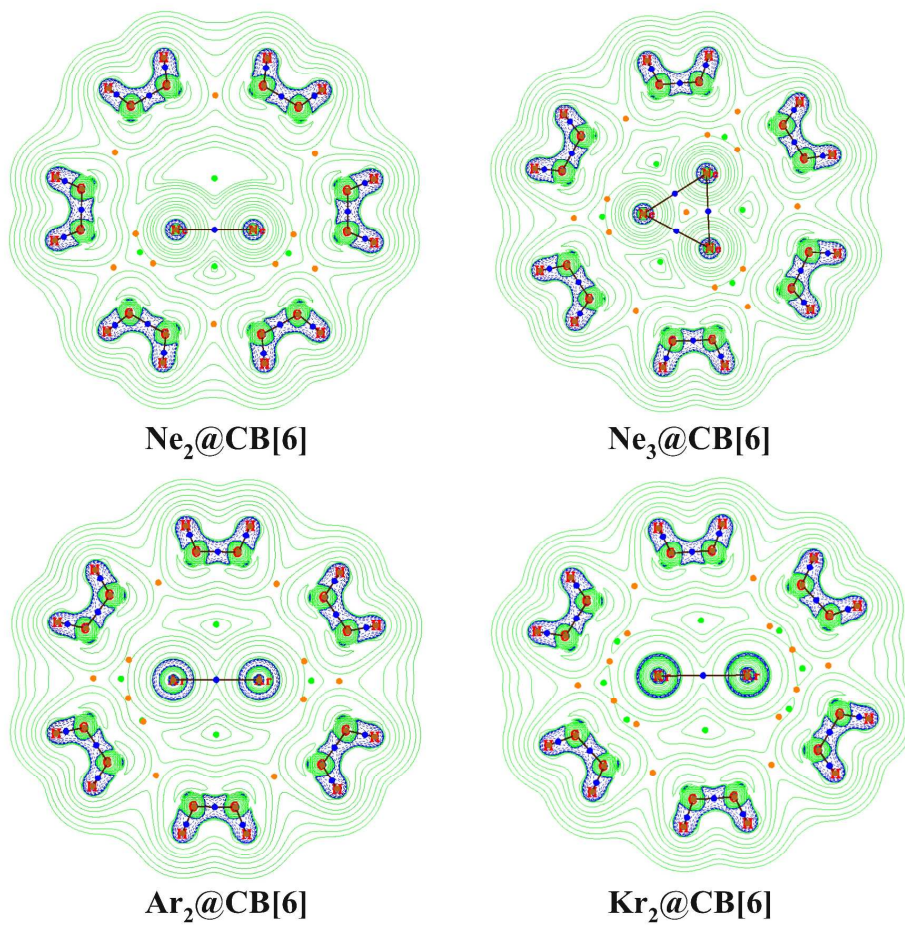


Figure 3. Contour plots of the Laplacian of the electron density of $\text{Ng}_n@\text{CB}[6]$ ($n = 2, 3$) systems computed at the $\omega\text{B97X-D}/6-311\text{G}(2\text{d},\text{p})$ level. (Green lines show the area of $\nabla^2\rho(\mathbf{r}) > 0$ whereas blue lines show the area of $\nabla^2\rho(\mathbf{r}) < 0$)

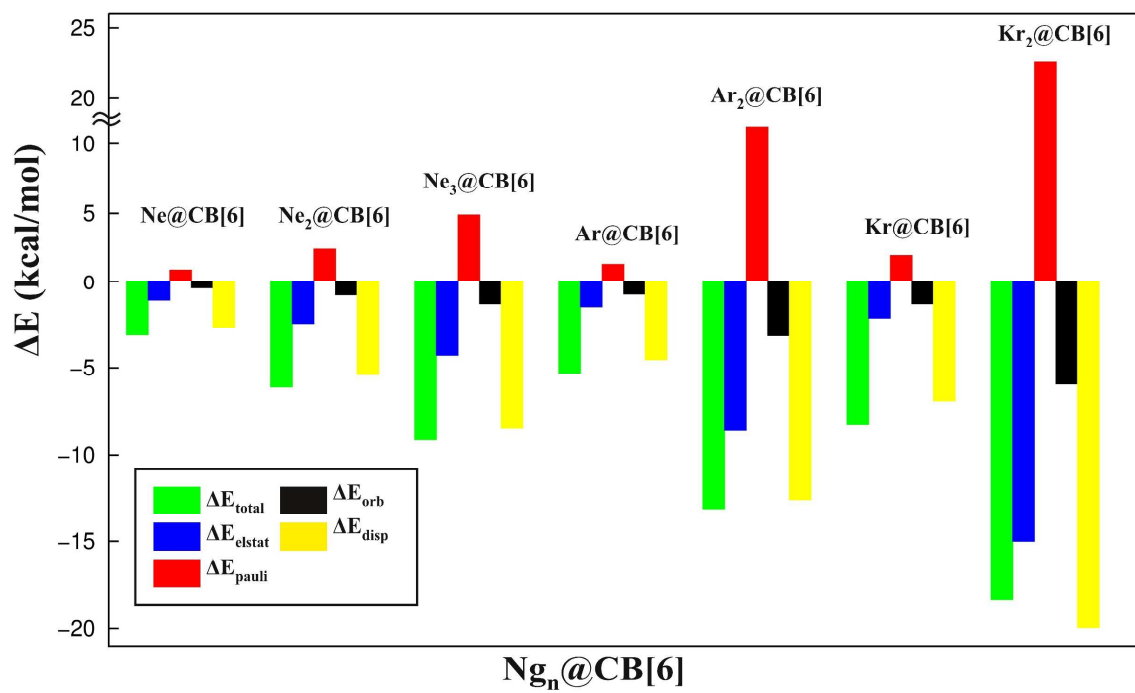


Figure 4. EDA results of the $\text{Ng}_n@\text{CB}[6]$ systems considering Ng_n as one fragment and $\text{CB}[6]$ as another fragment at the SSB-D/DZP// ω B97X-D/6-311G(2d,p) level.

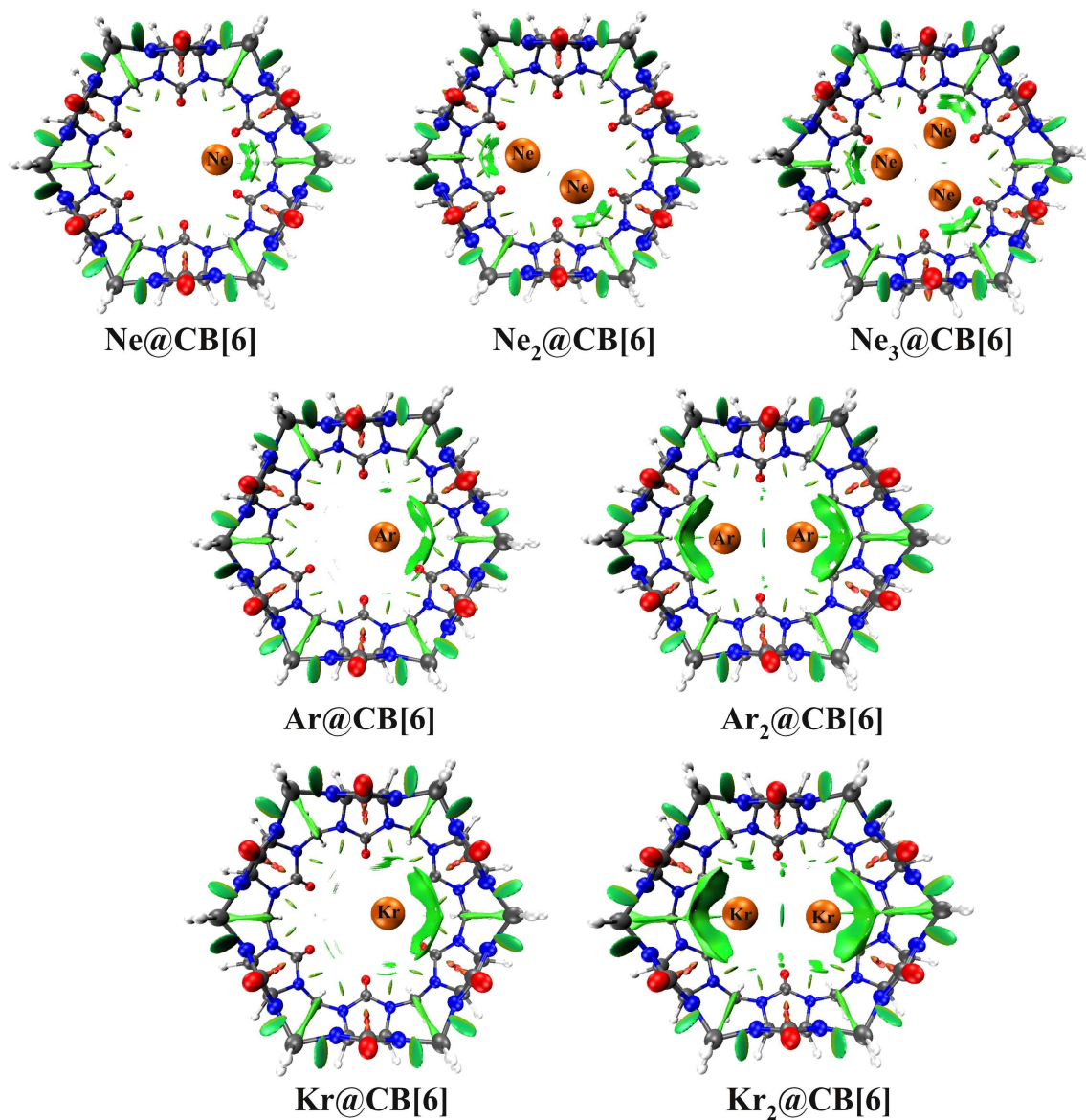


Figure 5. NCI isosurface plots of the $\text{Ng}_n@\text{CB}[6]$ systems.

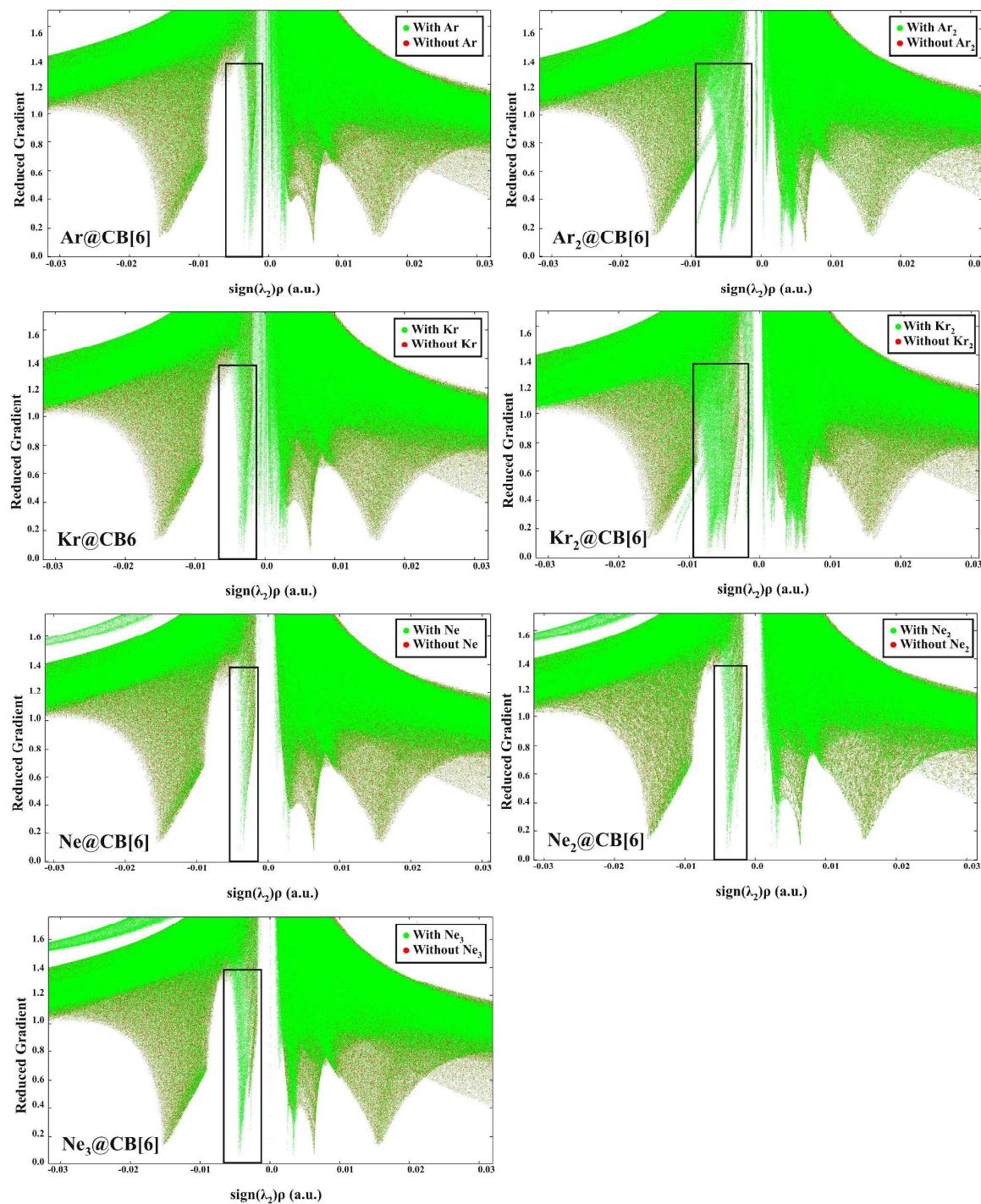


Figure 6. The zoomed view of the plots of reduced gradient versus $\text{sign}(\lambda_2)\rho$ of the $\text{Ng}_n@\text{CB}[6]$ systems

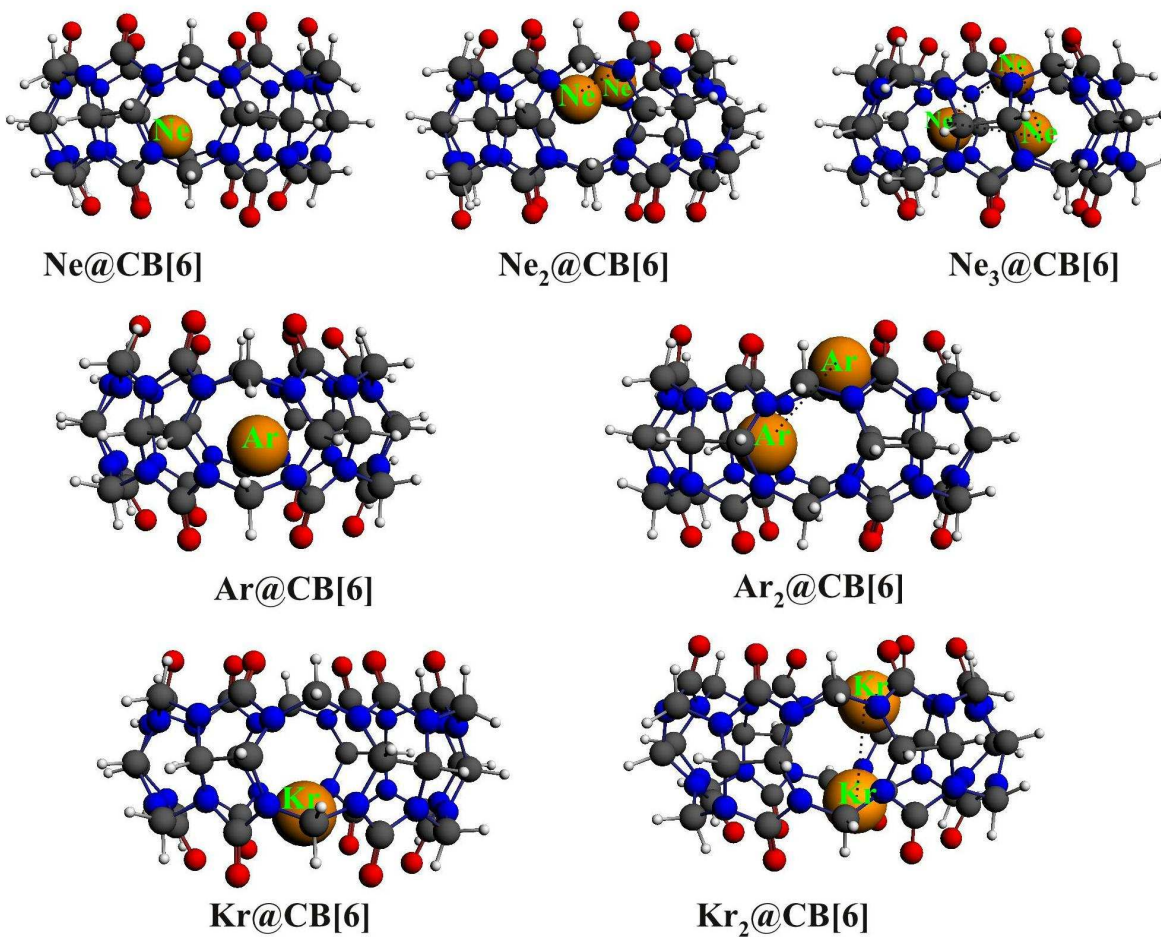


Figure 7. The resulting structures of Ng_n@CB[6] systems after 1 ps simulation at 298 K.

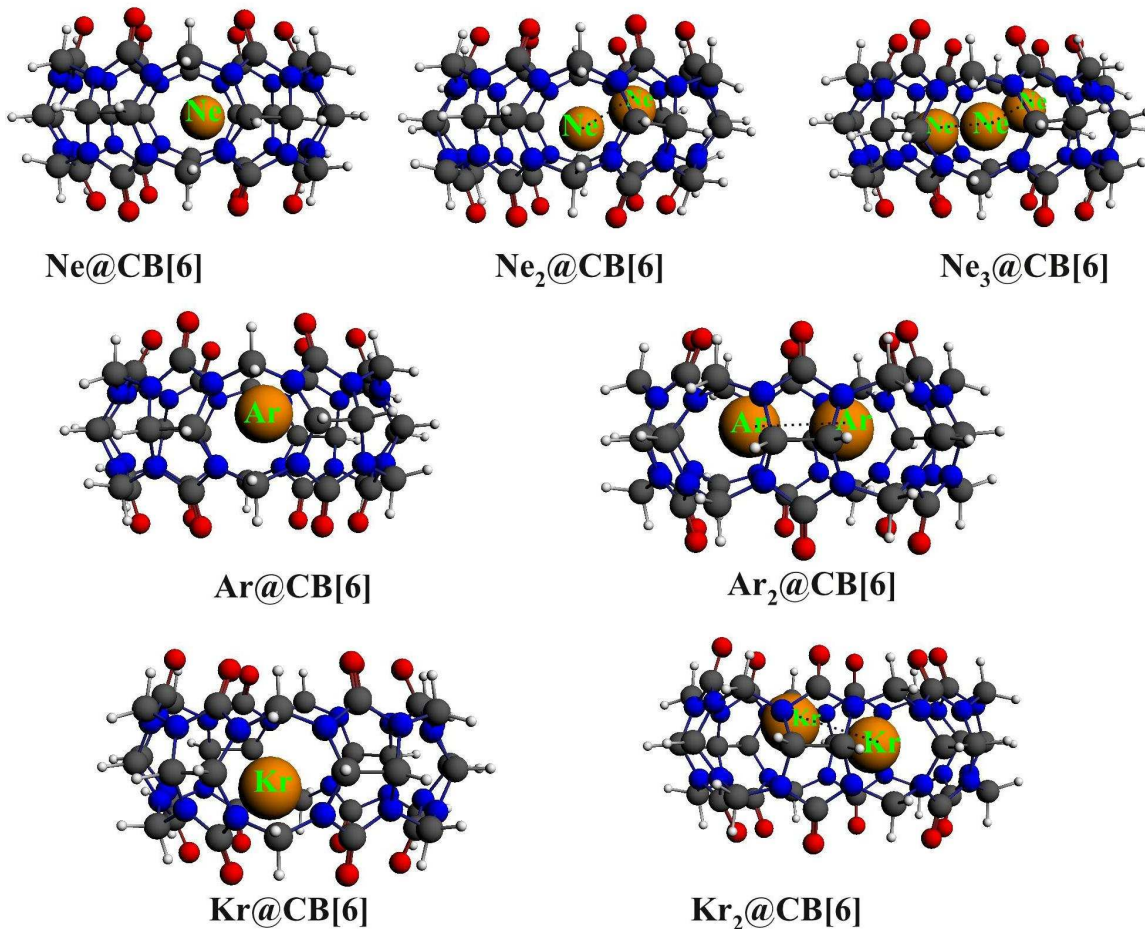


Figure 8. The resulting structures of Ng_n@CB[6] systems after 1 ps simulation at 77 K.

Tables

Table 1. Preparation energies (ΔE_{prep} , kcal/mol), total interaction energies (ΔE , kcal/mol), ZPE uncorrected dissociation energies (D_e , kcal/mol), ZPE corrected dissociation energies (D_0 , kcal/mol) and dissociation enthalpy (ΔH , kcal/mol) computed at the ω B97X-D/6-311G(2d,p) level.

Process	ΔE_{prep}	Process	ΔE	Process	D_e	D_0	ΔH	Gap
$\text{CB[6]} \rightarrow (\text{CB[6]})$	0.0	$\text{Ne} + (\text{CB[6]}) \rightarrow \text{Ne@CB[6]}$	-4.3	$\text{Ne@CB[6]} \rightarrow \text{Ne} + \text{CB[6]}$	4.3	3.4	4.0	10.78
$\text{CB[6]} \rightarrow (\text{CB[6]})$	0.1		-8.6					
$\text{Ne}_2 \rightarrow (\text{Ne}_2)$	0.0	$(\text{Ne}_2) + (\text{CB[6]}) \rightarrow \text{Ne}_2@\text{CB[6]}$	(-4.3)	$\text{Ne}_2@\text{CB[6]} \rightarrow \text{Ne} + \text{Ne@CB[6]}$	4.3	4.1	4.3	10.77
$\text{CB[6]} \rightarrow (\text{CB[6]})$	0.1							
$\text{Ne}_3 \rightarrow (\text{Ne}_3)$	0.0	$(\text{Ne}_3) + (\text{CB[6]}) \rightarrow \text{Ne}_3@\text{CB[6]}$	-12.8 (-4.3)	$\text{Ne}_3@\text{CB[6]} \rightarrow \text{Ne} + \text{Ne}_2@\text{CB[6]}$	4.4	3.9	4.0	10.77
$\text{CB[6]} \rightarrow (\text{CB[6]})$	0.1	$\text{Ar} + (\text{CB[6]}) \rightarrow \text{Ar@CB[6]}$	-4.7	$\text{Ar@CB[6]} \rightarrow \text{Ar} + \text{CB[6]}$	4.6	4.1	5.1	10.80
$\text{CB[6]} \rightarrow (\text{CB[6]})$	1.1		-8.3					
$\text{Ar}_2 \rightarrow (\text{Ar}_2)$	1.3	$(\text{Ar}_2) + (\text{CB[6]}) \rightarrow \text{Ar}_2@\text{CB[6]}$	(-4.2)	$\text{Ar}_2@\text{CB[6]} \rightarrow \text{Ar} + \text{Ar@CB[6]}$	1.5	1.0	0.4	10.77
$\text{CB[6]} \rightarrow (\text{CB[6]})$	0.0	$\text{Kr} + (\text{CB[6]}) \rightarrow \text{Kr@CB[6]}$	-7.4	$\text{Kr@CB[6]} \rightarrow \text{Kr} + \text{CB[6]}$	7.4	6.9	7.2	10.80
$\text{CB[6]} \rightarrow (\text{CB[6]})$	2.8		-12.3					
$\text{Kr}_2 \rightarrow (\text{Kr}_2)$	2.3	$(\text{Kr}_2) + (\text{CB[6]}) \rightarrow \text{Kr}_2@\text{CB[6]}$	(-6.2)	$\text{Kr}_2@\text{CB[6]} \rightarrow \text{Kr} + \text{Kr@CB[6]}$	0.2	-0.5	0.0	10.77

Table 2. The free energy change (ΔG , kcal/mol) for the dissociation processes computed at 298 K and 77 K.

Process	$\Delta G_{298\text{K}}$	$\Delta G_{77\text{K}}$	Process	$\Delta G_{298\text{K}}$	$\Delta G_{77\text{K}}$
$\text{Ne@CB[6]} \rightarrow \text{Ne} + \text{CB[6]}$	-2.1	2.5	$\text{Ne@CB[6]} \rightarrow \text{Ne} + \text{CB[6]}$	-2.1	2.5
$\text{Ne}_2@\text{CB[6]} \rightarrow \text{Ne} + \text{Ne@CB[6]}$	1.3	3.7	$\text{Ne}_2@\text{CB[6]} \rightarrow 2\text{Ne} + \text{CB[6]}$	-0.9	6.2
$\text{Ne}_3@\text{CB[6]} \rightarrow \text{Ne} + \text{Ne}_2@\text{CB[6]}$	-4.5	1.8	$\text{Ne}_3@\text{CB[6]} \rightarrow 3\text{Ne} + \text{CB[6]}$	-5.4	8.1
$\text{Ar@CB[6]} \rightarrow \text{Ar} + \text{CB[6]}$	-2.2	3.1	$\text{Ar@CB[6]} \rightarrow \text{Ar} + \text{CB[6]}$	-2.2	3.1
$\text{Ar}_2@\text{CB[6]} \rightarrow \text{Ar} + \text{Ar@CB[6]}$	-4.5	-0.5	$\text{Ar}_2@\text{CB[6]} \rightarrow 2\text{Ar} + \text{CB[6]}$	-4.5	2.6
$\text{Kr}@{\text{CB}}[6] \rightarrow \text{Kr} + \text{CB[6]}$	2.9	5.7	$\text{Kr}@{\text{CB}}[6] \rightarrow \text{Kr} + \text{CB[6]}$	2.9	5.7
$\text{Kr}_2@\text{CB[6]} \rightarrow \text{Kr} + \text{Kr@CB[6]}$	-12.1	-2.7	$\text{Kr}_2@\text{CB[6]} \rightarrow 2\text{Kr} + \text{CB[6]}$	-12.1	3.1

1
2
3
4
5
6
7
8
9
10 **Table 3.** Different topological descriptors at the BCPs of Ng-N or Ng-Ng bonds
11 computed at the ω B97X-D/6-311G(2d,p) level.
12
13

14
15

Systems	BCP	$\rho(r_c)$	$\nabla^2\rho(r_c)$	$G(r_c)$	$V(r_c)$	$H(r_c)$
Ne@CB[6]	Ne-N	0.003	0.019	0.004	-0.003	0.001
Ne ₂ @CB[6]	Ne-Ne	0.003	0.026	0.005	-0.003	0.002
	Ne-N	0.004	0.021	0.004	-0.003	0.001
Ne ₃ @CB[6]	Ne-Ne	0.003	0.026	0.005	-0.003	0.002
	Ne-N	0.004	0.022	0.004	-0.003	0.001
Ar@CB[6]	Ar-N	0.003	0.011	0.002	-0.001	0.001
Ar ₂ @CB[6]	Ar-Ar	0.009	0.041	0.008	-0.006	0.002
	Ar-N	0.006	0.022	0.004	-0.003	0.001
Kr@CB[6]	Kr-N	0.003	0.012	0.002	-0.002	0.000
Kr ₂ @CB[6]	Kr-Kr	0.012	0.044	0.009	-0.008	0.001
	Kr-N	0.007	0.024	0.005	-0.004	0.001

TOC

